J Electr Eng Technol Vol. 8, No. 2: 385-392, 2013
http://dx.doi.org/10.5370/JEET.2013.8.2.385

ISSN(Print) 1975-0102
ISSN(Online) 2093-7423

Uncalibrated Visual Servoing through the Efficient Estimation of the Image Jacobian for Large Residual

Gon-Woo Kim†

Abstract – An uncalibrated visual servo control method for tracking a target is presented. We define the robot-positioning problem as an unconstrained optimization problem to minimize the image error between the target feature and the robot end-effector feature. We propose a method to find the residual term for more precise modeling using the secant approximation method. The composite image Jacobian is estimated by the proper method for eye-to-hand configuration without knowledge of the kinematic structure, imaging geometry and intrinsic parameter of camera. This method is independent of the motion of a target feature. The algorithm for regulation of the joint velocity for safety and stability is presented using the cost function. Adaptive regulation for visibility constraints is proposed using the adaptive parameter.

Keywords: Image jacobian, Uncalibrated visual servoing, Target tracking, Visibility constraints.

1. Introduction

Visual servoing is a control method that uses visual information. Visual-feedback control is generally referred to as visual servoing. According to the feedback information, the visual servo control systems can be divided into two by taxonomy of visual servo systems proposed by Sanderson and Weiss [1]. These two well-known systems are the position-based and the image-based visual servo control system.

Image-based visual servoing is generally robust not only with respect to camera but also to robot calibration error. In the image-based visual servoing for tracking a target, the image error between the target feature and the end-effector (or desired target feature) is used to control the robot manipulator [1-8]. In this paper, the robot system is controlled using nonlinear least squares optimization method based on unconstrained optimization problem for the image error. Jagersand [8] and Piepmeier [5, 6, 9] presented the image-based visual servoing using the nonlinear least squares optimization method, but they did not use the residual term due to the difficulty in estimating (zero residual case).

This paper proposes the image-based visual servoing method in which the estimation of the residual term has been modified using the secant approximation method (large residual case). The dynamic visual servoing method was adopted for moving targets [9].

The image Jacobian contains system parameters such as the kinematic model and the camera model. The system parameters can be identified in a calibration process. With this process, the visual servo controller using the image Jacobian with this process is not robust for disturbance, change of parameters and so on. To overcome such defects, the uncalibrated visual servoing using the estimation of the image Jacobian was presented [4, 6, 8-15]. Estimating the image Jacobian using the Broyden's method was originally developed by Hosoda [4]. In [5], the authors demonstrated the model-independent target tracking using the extended methods of estimation of the image Jacobian. Hosada [4] and Jagersand [8] demonstrated the estimation of the image Jacobian using the Broyden's method for a stationary target, and Piepmeier [6, 9] proposed the dynamic Jacobian estimation method for a moving target. Shademan et al. in [14] proposed the robust Jacobian estimation algorithm with the rejection of outliers using M-estimator. Wang et al. proposed the adaptive visual servoing for the eye-in-hand robot system using point and line features [15].

Most of the previous works [4, 6, 8, 9, 11] used the image error to estimate the image Jacobian using the Broyden's method, but it is dependent for the target feature. The proposed algorithm to estimate the image Jacobian in this paper is mostly based on the algorithm presented in [11]. For the moving target, however, the previous work has a little but crucial problem caused by the affine model using not the end-effector feature but the image error. Therefore we propose an improved Jacobian estimation method in this paper. We defined the affine model for the end-effector feature and we estimated the image Jacobian with the affine model. This method is efficient for the eye-to-hand visual servoing and independent of the target feature irrespective of whether the target is moving or not. We also evaluate the improved performance using the experimental results.

The control input should be regulated for safety purpose in real experiments because the end-effector can move beyond the visual scope of the camera in the eye-to-hand

† Corresponding Author: School of Electronics Engineering, Chung buk National Univerity, Korea.(gwkim@cbnu.ac.kr)
Received: January 20, 2012; Accepted: December 10, 2012

robot system. We propose, however, the regulation method using the cost function approach considering the visibility in the image plane. In several papers, the cost function approach has been applied to avoid the robot joint limits [12, 13]. This paper uses the concept of the cost function and defines the cost function to regulate the joint velocity using the adaptive parameter for the visibility constraints.

There are two major contributions of this paper. The first is that the estimation method of the image Jacobian has been improved using the affine model for the end-effector feature. The second is that a method for regulating the joint velocity using the adaptive parameter for the visibility constraints is proposed.

The discussion in this paper will proceed as follows. Section II presents the background of the proposed uncalibrated image-based visual servoing with the modified method for estimating the image Jacobian. Section III shows the regulation algorithm of the joint velocity using the cost function. The experimental results are given in Section IV.

2. Background

2.1 Unconstrained optimization problem for image-based visual servoing

Considering the eye-to-hand vision system, the camera can observe the target feature and the end-effector feature at the same time. In the image plane, the moving target feature, $f_t(t)$, is defined as the function of time t, and the end-effector feature, $f_r(q)$, is defined as the function of the robot joint variables q. The control problem of the target tracking is defined as the minimization of the image error. The image error between the moving target feature and the end-effector feature can be expressed as $e(q,t) = f_r(q) - f_t(t)$ in the image plane. In order to minimize the image error, we define the objective function as

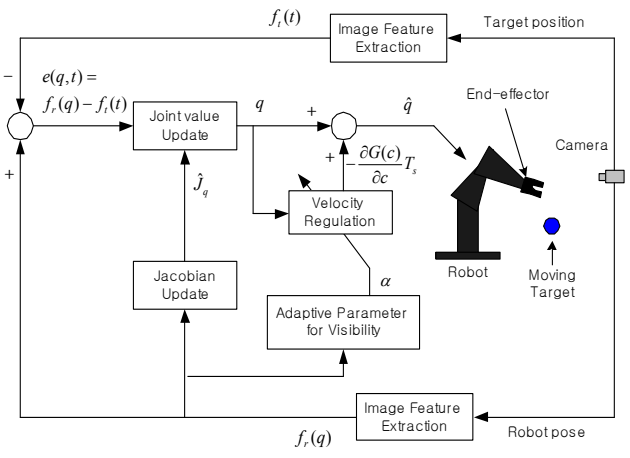

Fig. 1. The schematic control architecture for eye-to-hand visual servo control system

$$E(q,t) = \frac{1}{2} e^T(q,t) e(q,t) \tag{1}$$

This objective function is a highly nonlinear function because the image features are determined by the complex geometric relationship.

The nonlinear least squares optimization problem for tracking a moving target can be defined as

$$\min_{q \in R^n} E(q,t) \tag{2}$$

which is minimized at the robot joint configuration q^* satisfying the equation, $\partial E(q^*)/\partial q = \mathbf{0}$.

If we assume the linear model in the neighborhood at $(\bar{q}, \bar{t})$, the objective function can be approximated using the Taylor series expansion for multivariable functions as

$$\hat{E}(q,t) = E(\bar{q},\bar{t}) + \nabla_q E(q,t)(q-\bar{q}) + \nabla_t E(q,t)(t-\bar{t}) \tag{3}$$

where ∇_q and ∇_t are partial derivatives of variable q and t, respectively.

Assume that the objective function is the second order differentiable for q. The gradient of the approximation model is shown as

$$\begin{aligned} \frac{\partial \hat{E}(q,t)}{\partial q} &= \nabla_q E(\bar{q},\bar{t}) + \nabla_q^2 E(\bar{q},\bar{t})(q-\bar{q}) \\ &\quad + \nabla_q \left(\nabla_t E(\bar{q},\bar{t}) \right)(t-\bar{t}) \end{aligned} \tag{4}$$

We define the composite image Jacobian of robot, $J_q(q) = \partial f_r(q)/\partial q$ and the image Jacobian of target, $J_t(t) = \partial f_t(t)/\partial t$. The first and second order differential terms of the objective function are shown as

$$\begin{aligned} \nabla_q E(q) &= J_q(q)^T e(q,t) \\ \nabla_q^2 E(q) &= J_q(q)^T J_q(q) + R(q,t) \end{aligned} \tag{5}$$

where $R(q,t) = \nabla_q \left(J_q(q) \right)^T e(q,t)$

If the gradient of the approximation model at (q_k, t_k) is zero, the robot joint configuration can be the minimizer of the object function. The iterative form of the joint value to minimize the objective function become

$$\begin{aligned} q_{k+1} &= q_k - (J_q(q_k)^T J_q(q_k) + R(q_k,t_k))^{-1} \\ &\quad \cdot J_q(q_k)^T \left(e(q_k,t_k) + J_t(t_k) T_s \right) \end{aligned} \tag{6}$$

where T_s is the time period which is a constant. For the static target, the image Jacobian of the target, $J_t(t)$, is zero.

We propose the method to estimate the residual term for more precise modeling using the secant approximation method.

We have to compute the Hessian matrix of the robot end-effector feature vector, $H(q) = \nabla_q^2 f_r(q)$, in order to find the gradient of the composite image Jacobian of robot.

Using the secant approximation method, the approximation model of the Hessian matrix at q_k, H_k, can be expressed as

$$\begin{aligned} H_k\left(q_k - q_{k-1}\right) &= \nabla_q f_r(q_k) - \nabla_q f_r(q_{k-1}) \\ &= J_q(q_k) - J_q(q_{k-1}) \end{aligned} \tag{7}$$

The approximation model can be adopted as the Hessian matrix in (5), that is, $H_k \approx \nabla_q^2 f_r(q_k)$ at q_k.

$$R\left(q_k, t_k\right) = \frac{\left(J_q(q_k) - J_q(q_{k-1})\right)^T e(q_k)\left(q_k - q_{k-1}\right)^T}{\left(q_k - q_{k-1}\right)^T\left(q_k - q_{k-1}\right)} \tag{8}$$

2.2 Estimation of the image jacobian

In this section, the proper algorithm of estimating the image Jacobian for eye-to-hand vision system is presented. We used only the robot end-effector feature for estimating the image Jacobian. This method shows better performance than the previous works [4, 6, 8, 9, 11] and can be applied for both a stationary target and a moving target.

The proposed algorithm to estimate the image Jacobian in this paper is mostly based on the algorithm presented in [11]. For the moving target, however, the previous work has a little but crucial problem caused by the affine model using not the end-effector feature but the image error. Therefore, we proposed the modified image Jacobian estimation method independent of the target feature for eye-to-hand visual servoing.

The Taylor series expansion of the robot end-effector feature near q_k, can be expressed as

$$f_r(q) = f_r(q_k) + \nabla_q f_r(q_k)(q - q_k) + O\left(\left\|q - q_k\right\|^2\right) \tag{9}$$

We approximate (9) by ignoring the high-order term and define the affine model of the robot end-effector feature as

$$l_k(q) = f_r(q_k) + \nabla_q f_r(q_k)(q - q_k) \tag{10}$$

This affine model is more efficient than the other affine models used in the previous work. If the *k*th affine model correctly specifies the error at the (*k-1*)th increment, the equation can be calculated from (10).

$$(\hat{J}_q(q_k) - \hat{J}_q(q_{k-1}))\Delta q = \left(f_r(q_k) - f_r(q_{k-1})\right) - \hat{J}_q(q_{k-1})\Delta q \tag{11}$$

The estimated image Jacobian can be calculated using the Broyden's rank-one update method as follows.

$$\begin{aligned} \hat{J}_q(q_k) &= \hat{J}_q(q_{k-1}) \\ &+ \frac{\left(f_r(q_k) - f_r(q_{k-1}) - \hat{J}_q(q_{k-1})\left(q_k - q_{k-1}\right)\right)\left(q_k - q_{k-1}\right)^T}{\left(q_k - q_{k-1}\right)^T\left(q_k - q_{k-1}\right)} \end{aligned} \tag{12}$$

We applied the modified estimation method using recursive least squares (RLS) algorithm. The cost function for a change of the affine model in (10) can be expressed as

$$C(k) = \sum_{i=1}^{n} \lambda^{k-i} \left\| l_k(q_{i-1}) - l_{i-1}(q_{i-1}) \right\|^2 \tag{13}$$

$\hat{J}_q(q_k)$ is calculated to minimize (13) using RLS algorithm. That is

$$\begin{aligned} \hat{J}_q(q_k) &= \hat{J}_q(q_{k-1}) \\ &+ \frac{\left(f_r(q_k) - f_r(q_{k-1}) - \hat{J}_q(q_{k-1})\left(q_k - q_{k-1}\right)\right)\left(q_k - q_{k-1}\right)^T P_k}{\lambda + \left(q_k - q_{k-1}\right)^T P_k \left(q_k - q_{k-1}\right)} \\ P_k &= \frac{1}{\lambda}\left(P_{k-1} - \frac{P_{k-1}\left(q_k - q_{k-1}\right)\left(q_k - q_{k-1}\right)^T P_{k-1}}{\lambda + \left(q_k - q_{k-1}\right)^T P_{k-1}\left(q_k - q_{k-1}\right)}\right) \end{aligned} \tag{14}$$

The forgetting factor, $\lambda \in [0,1]$, is the rate of dependency for the past data. As it is already known, the factor greatly influences the performance of the system.

3. Regulation of the Joint Velocity

In this section, we propose the velocity regulation algorithm for safety and stability purpose. The adaptive parameter adjusts the velocity regulation level for the visibility constraints in the image plane.

If the velocity of the joint value calculated in (6) is so large to the extent that the robot end-effector moves beyond the visible scope of the camera, the camera would lose sight of the position of the robot end-effector. This is in turn means that the visual servo control has failed. Normally the joint velocity is regulated using the heuristic method to ensure safety. However, we propose an efficient method for regulation using cost function of the joint velocity and adaptive parameter for visibility constraints.

3.1 Adaptive parameter for visibility constraints

The visibility constraints are increased near the boundary of the image plane. Therefore it is necessary to regulate the image feature velocity of the robot end-effector near the boundary more tightly than the center.

We define the adaptive parameter for consideration to these visibility constraints.

$$\alpha = (1-\gamma)\exp\left(-\frac{1}{2}(f_r(q)-f_p)^T W(f_r(q)-f_p)\right)+\gamma \quad (15)$$
$$for \quad 0 \le \gamma < 1$$

where γ is a positive scaling factor which adjusts the lower bound of the image feature velocity of the robot end-effector and W is a weighting matrix which is a positive definite matrix. f_p is the principle point of the image plane, that is, the center point of the image plane in pixels.

As shown in Fig. 2, the value of the adaptive parameter is almost 1 near the center and (1- γ) near the boundary where γ is 0.2. The sharpness of the ridge of the adaptive parameter is determined by a weighting matrix, W. The adaptive parameter for the visibility constraints is used as a scaling factor for the cost function to prevent the joint velocity from exceeding the limit of feature velocity.

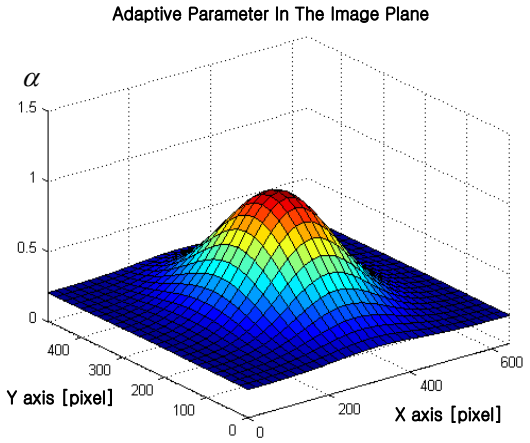

Fig. 2. Adaptive parameter for visibility constraints: γ=0.2, W=10-4×I2 and fp = [320 240]T

3.2 Cost function for regulation of the joint velocity using the adaptive parameter

In this paper, the cost function is defined using the square of the joint velocity. This cost function is intended to regulate the joint velocity to prevent it from exceeding the limit of the joint velocity and to modify the control input of the robot joint value using the minimizer of the cost function.

The cost function to be minimized is defined by

$$\min_c G(c) = \frac{1}{2}c^T c$$
$$where\ c = \begin{bmatrix} c^1 \\ c^2 \\ \vdots \\ c^n \end{bmatrix},\quad c^j = \begin{cases} \dot{q}^j - \alpha\dot{q}^j_{\mathbf{limit}} & \mathbf{for}\ \dot{q}^j > \dot{q}^j_{\mathbf{limit}} \\ \dot{q}^j + \alpha\dot{q}^j_{\mathbf{limit}} & \mathbf{for}\ \dot{q}^j < -\dot{q}^j_{\mathbf{limit}} \\ \mathbf{0} & otherwise \end{cases} \quad (16)$$

where α is the adaptive parameter, $\dot{q}$ is the joint velocity and $\dot{q}_{\mathbf{limit}}$ is the limit of the joint velocity. The offset region is between $-\alpha\dot{q}_{\mathbf{limit}}$ and $\alpha\dot{q}_{\mathbf{limit}}$ as shown in Fig. 3. Fig. 3 shows the cost function when the image feature of the robot end-effector is located at the center of the image plane. Within the offset region, the visual tracking system is not disturbed by the cost function.

To minimize the cost function for the joint velocity, the gradient of the cost function must be zero

$$\nabla_c G(c) = \frac{\partial G(c)}{\partial c} = \mathbf{0} \quad (17)$$

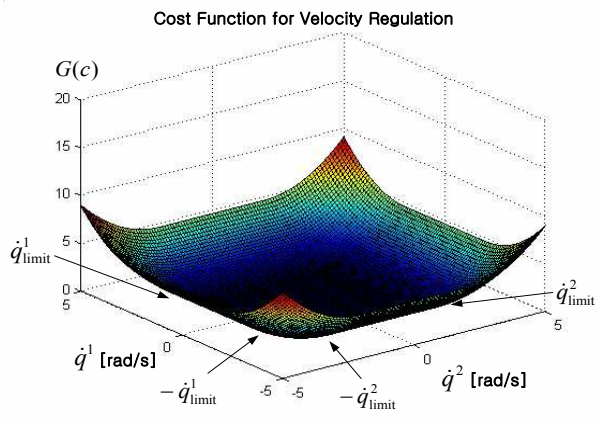

Fig. 3. The cost function, G(c), for regulation of the joint velocity at the case of two joints: $\dot{q}_{\mathbf{limit}} = [\mathbf{1.5}\ \ \mathbf{1.5}]^T$ rad/s

In order for the gradient of the cost function to be zero, the joint velocity must be controlled to move in opposite direction of the gradient. Then, we can find the joint value to minimize the cost function and modify the joint value to the iterative form as

$$q_{k+1} = q_k - \frac{\partial G(c)}{\partial c}\cdot T_s \quad (18)$$

where T_s is the time period.

In Section II, we found the iterative form of joint value for minimizing the objective function for tracking a moving target. Here, we will consider two tasks: one is tracking a moving target using the objective function mentioned in Section II, and the other is regulating the joint velocity using the cost function in this section.

In order to control the robot end-effector properly, a process to combine these two tasks is needed. Using (6) and (18), the modified iterative form of the joint value becomes

$$q_{k+1} = q_k - (J_q(q_k)^T J_q(q_k) + R(q_k,t_k))^{-1} \cdot J(q_k)^T \left(e(q_k,t_k) + J_t(t_k)T_s\right) - \frac{\partial G(c)}{\partial c}\cdot T_s \quad (19)$$

3.3 Simulation of the regulation of the joint velocity using the adaptive parameter

For the eye-to-hand system, the robot should not be controllable if the end-effector moves out of the view of the camera. It is because the pose information of the end-effector has been lost.

For evaluating the effectiveness of the regulation of the joint velocity, we performed the simulation. We assume that the resolution of the camera is 640x480(pixel). For the effective evaluation of performance, the stationary goal position is set as (450, 480) at the boundary in the image plane as shown in Fig. 4 and 5.

Fig. 4 shows the simulation result without the regulation of the joint velocities using (6). As you can see at the top of Fig. 4, the end-effector has been disappeared in the view of the camera while it is approaching to the goal position. (In this simulation, we provide the pose information of the end-effector even if the end-effector stays out of the view.) In this situation, there is little possibility to succeed the visual servoing task of the end-effector toward the goal position.

For the same situation, however, the joint velocity can be effectively regulated using the proposed regulation algorithm as shown in Fig. 5. Near the boundary in the image plane, the end-effector has been controlled properly using the proposed algorithm in order to stay it within the view of the camera. Fig. 5. (*top*) shows the trajectory of the end-effector. In this result, we verified the efficiency for overcoming the visibility constraints.

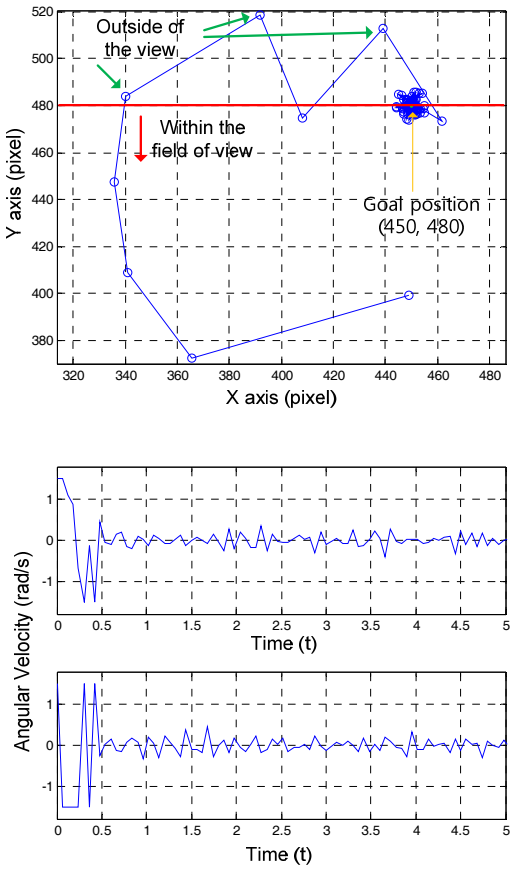

Fig. 4. Simulation result without the regulation of the joint velocities: trajectory of the end-effector (*top*), joint velocities (*bottom*)

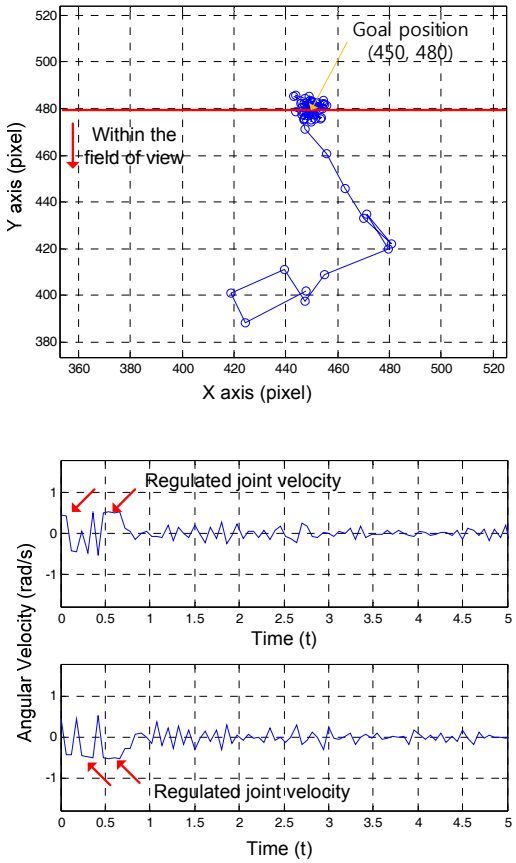

Fig. 5. Simulation result with the proposed regulation of the joint velocities: trajectory of the end-effector (*top*), joint velocities (*bottom*)

4. Experimental Results

The proposed methods were applied on the 3DOF SNU-ERC DD (Direct Drive) planar robot for the eye-to-hand configuration. However, we used only two links out of the three and did not consider the redundant control in order to simplify the problem.

In this section, we performed experiments for two cases. In Section V-A, we explain the experiment that was performed for the algorithm to find the residual term for large residual. Through this experiment, we proved the validity of the algorithm by comparing the large residual case with the zero residual case. In Section V-B, the estimation algorithm of the image Jacobian using the affine model for the end-effector feature was applied. The experimental results for the estimation algorithm were then

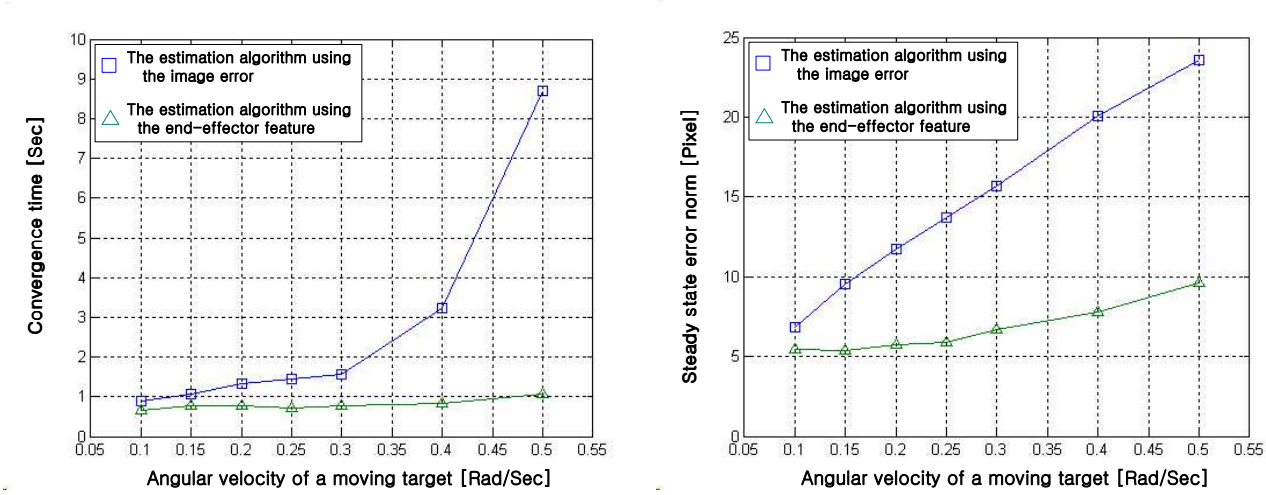

(a) (b)

Fig. 6. Comparisons of the estimation of the image Jacobian between the algorithm using the image error and the algorithm using the end-effector feature. (a) The convergence time for tracking a moving target (b) The average steady-state error norm for tracking a moving target: The motion of the target is (320-200sin (2πωt), 240+100cos (2πωt)) and the angular velocity of a moving target is ω.

compared with the previous works [5, 6]. Finally, we applied the algorithm to regulate the joint velocity using the adaptive parameter for visibility constraints in these experiments.

The 3DOF SNU-ERC DD robot was used for testing these algorithms. The vision system used Teli CS6100 CCD camera and the Meteor II frame grabber manufactured by Matrox in order to obtain the digital image. The resolution of the camera was 640×480 (1 pixel ≈ 0.5*mm*). The frame grabber was installed in a Pentium II 800MHz PC running the Windows NT 4.0 operating system. The sampling period was 60*ms*.

The initial image Jacobian at t=0, $\hat{J}_q(q_0)$, was the 2x2 identity matrix, I_2. We used the value of $\lambda = 0.5$ until convergence was achieved and then changed the value for $\lambda = 0.9$. The limit of the joint velocity in (16) was chosen to be $[1.5\ 1.5]^T$ (rad/s) using the heuristic method. We had to consider several characteristics such as the field of view, kinematics, and the configuration of the robot in order to choose the limit of the joint velocity properly. The adaptive parameter for visibility constraints, $\gamma = 0.5$, $W = 10^{-4}\times I_2$ and $f_p = [320\ 240]^T$ was applied.

The initial position of the robot end-effector for these experiments was set as (450, 400). For a stationary target, the position of the target in the image plane was (150, 150) pixel. For a moving target, we used a virtual moving target instead of the real moving target. The motion of the target was (320 − 200sin ($2\pi\omega t$) + n, 240 + 100cos ($2\pi\omega t$) + n) with an initial position at (320, 340) in the image plane. The angular velocity, ω (rad/s), was used to change the speed of the motion of the virtual moving target. The zero mean white Gaussian noise with variance of 4 pixels, n, was added to the motion of the target as the image processing noise.

In this experiment, we evaluated the performance of the system applying the estimation algorithm of the image Jacobian using the affine model for the end-effector feature. The experimental results using the proposed algorithm were compared with the results using the estimation algorithm of the image Jacobian using the image error, that is, the distance between the end-effector feature and the target in the image plane. The experiments were performed for a moving target.

For a moving target, the overall performance according to the motion of a moving target is shown in Fig. 6. The motion of the target is (320 − 200sin ($2\pi\omega t$) + n, 240 + 100cos ($2\pi\omega t$) + n) with the initial position at (320, 340) in the image plane. The angular velocity, ω (rad/s), was used to change the speed of the motion of the moving target.

As shown in Fig. 6(a), as the angular velocity is increased, the convergence time for the estimation algorithm using the image error is increased exponentially, but the convergence time for the proposed algorithm is slightly increased. This is because the proposed algorithm using the end-effector feature is not affected by the motion of a moving target. In one of the definitions of the image Jacobian, the proposed algorithm using the end-effector feature for the estimation of the image Jacobian is more suitable than the estimation algorithm using the image error. For the average steady-state error norm, the proposed algorithm also shows a better performance than the estimation algorithm using the image error as demonstrated in Fig. 6(b). As the angular velocity is increased, the average steady-state error norm is increased. The average steady-state error norms for the proposed algorithm are smaller than the average steady-state error norms for the estimation algorithm using the image error. Fig. 8(b) shows that the increase of the error norm for the proposed algorithm is slower than the increase

of the error norm for the estimation algorithm using the image error. These experimental results show that the proposed algorithm is more efficient for tracking a moving target than the estimation algorithm using the image error. This is because the proposed algorithm for estimating the image Jacobian is independent of a target feature.

Fig. 7 and 8 show the experimental results for the estimation algorithm using the image error and the estimation algorithm using the end-effector feature when the angular velocity is 0.3 rad/s. For the estimation algorithm using the image error, the convergence time is 1.56 sec (26 iterations) and the average steady-state error norm is 15.6837. For the proposed algorithm, however, the convergence time is 0.78 sec (13 iterations) and the average steady-state error norm is 6.6733.

In Fig. 7, the error norm is noisier than the error norm in Fig. 8. As the angular velocity of the moving target is increased, the image error is increased at the sample time. Therefore, the estimation algorithm using the image error is largely affected by the angular velocity. In the proposed algorithm, the target feature is not used for the estimation of the image Jacobian. Therefore, the target feature is only used for the nonlinear least squares optimization method.

The cyclic errors exist in Fig. 8(a) and the cyclic period is about 1.67 sec. As the angular velocity of the moving target is increased, the cyclic error is increased and becomes more apparent. These cyclic errors are produced by the moving target. Fig. 8(b) shows the trajectory until 3.3 sec. The motion of the moving target at 0.834 and 2.5 sec is decreased in the image plane because the moving target movies in a circular motion. Therefore, the error norm is decreased at $t = (n+1)\pi/2\omega$, $n = 0,1,2,\ldots$.

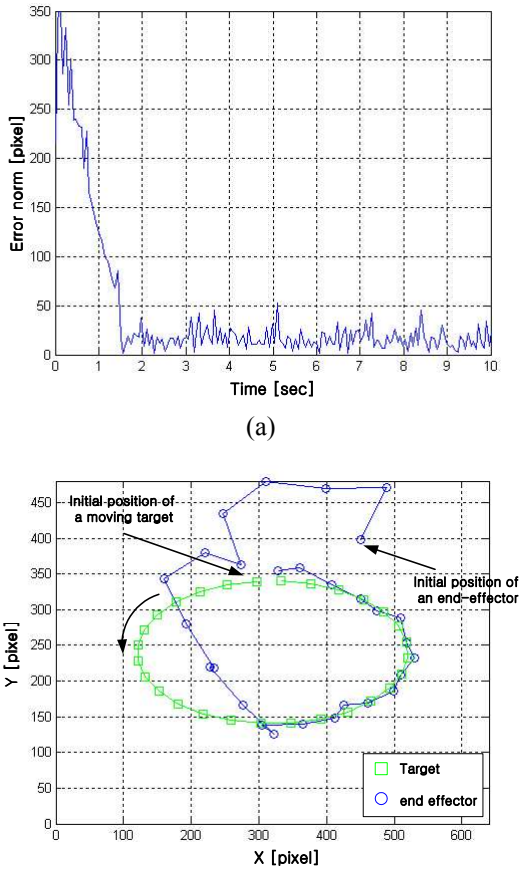

Fig. 7. Experimental results of the estimation of the image Jacobian using the image error at ω = 0.3 rad/s. (a) Pixel error norm for tracking a moving target.; (b) Trajectory of the end-effector feature and the moving target in the image plane: the convergence time is 1.56 sec (26 iterations), and the average steady-state error is 15.6837 pixels.

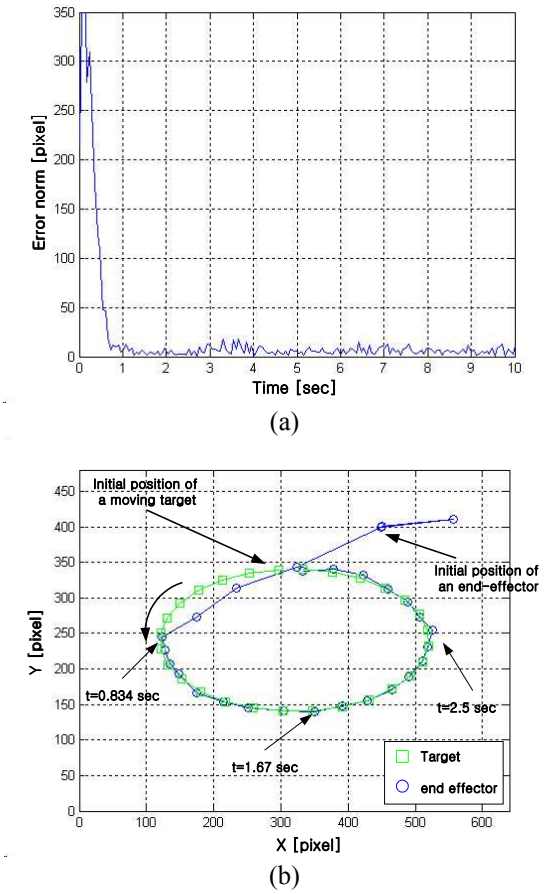

Fig. 8. Experimental results of the estimation of the image Jacobian using the end-effector feature at ω = 0.3 rad/s. (a) Pixel error norm for tracking a moving target; (b) Trajectory of the end-effector feature and the moving target in the image plane: the convergence time is 0.78 sec (13 iterations), and the average steady-state error is 6.6733 pixels.

5. Conclusion

In this paper, we proposed the uncalbrated visual servoing algorithm. The proposed algorithm was found to

be efficient for tracking a moving target in eye-to-hand configuration.

A nonlinear least squares optimization problem was defined for a calibration-free visual servo system, and the control system was proposed to minimize the image error. The Broyden's method was used for estimating the image Jacobian. In order to improve the stability of the system, a recursive least squares (RLS) algorithm was applied. We assumed a large residual for the model of an objective function. Therefore, we proposed this method to find the residual term using the secant approximation method.

We also proposed an algorithm for the estimating the image Jacobian using the end-effector feature. This algorithm is independent of the target feature, and in that respect it is efficient for tracking a stationary and a moving target.

To regulate the joint velocity for safety, the method using the cost function using the adaptive parameter for visibility constraints was proposed.

Lastly, we confirmed the validity for the proposed methods through experiments. We also verified that a large residual performs better than that of a zero residual for the convergence time as shown in the experimental results. Further, we found the estimation algorithm of the image Jacobian using the end-effector feature is more efficient than the estimation algorithm using the image error.

Acknowledgements

The authors acknowledge the financial support of the project 'Development of inspection equipment technology for harbor facilities' funded by Korea Ministry of Land, Transportation, and Maritime Affairs.

References

[1] A. C. Sanderson, and L. E. Weiss, "Image-based visual servo control using relational graph error signals," in *Proc. IEEE*, pp. 1074-1077, 1980.

[2] A. C. Sanderson, L. E. Weiss, and C. P. Neuman, "Dynamic sensor-based control of robots with visual feedback," *IEEE Trans. Robot. Automat.*, Vol. RA-3, pp. 404-417, Oct. 1987.

[3] H. Sutanto, R. Sharma, and V. Varma, "Image based autodocking without calibration," in *Proc. IEEE Int. Conf. Robotics and Automation*, pp. 974-979, 1997.

[4] K. Hosoda, and M. Asada, "Versatile visual servoing without knowledge of true Jacobian," in *Proc. IEEE/RSJ/GI Int. Conf. Intelligent Robots and Systems*, pp. 186-193, 1994.

[5] J. A. Piepmeier, G. V. McMurray, and H. Lipkin, "Tracking a moving target with model independent visual servoing : a predictive estimation approach," in *Proc. IEEE Int. Conf. Robotics and Automation*, pp. 2652-2657, 1998.

[6] J. A. Piepmeier, G. V. McMurray, and H. Lipkin, "A dynamic Jacobian estimation method for uncalibrated visual servoing," in *Proc. IEEE/ASME Int. Conf. Advanced Intelligent Mechatronics*, pp. 944-949, 1999.

[7] G. W. Kim, and B. H. Lee, "Efficient regulation of joint velocity in uncalibrated visual servoing," in *Proc. IEEE/ASME Int. Conf. Advanced Intelligent Mechatronics,* pp. 993-998, 2003.

[8] M. Jagersand, O. Fuentes, and R. Nelson, "Experimental evaluation of uncalibrated visual servoing for precision manipulation," in *Proc. IEEE Int. Conf. Robot. Automat.*, pp. 2874-2880, 1997.

[9] J. A. Piepmeier, G. V. McMurray, and H. Lipkin, "A dynamic quasi- Newton method for uncalibrated visual servoing," in *Proc. IEEE Int. Conf. Robotics and Automation*, pp. 1595-1600, 1999.

[10] M. Asada, T. Tanaka, and K. Hosoda, "Adaptive binocular visual servoing for independently moving target tracking," in *Proc. IEEE Int. Conf. Robotics and Automation*, pp. 2076-2081, 1997.

[11] G. W. Kim, B. H. Lee, and M. S. Kim, "Uncalibrated visual servoing technique using large residual," in *Proc. IEEE Int. Conf. Robotics and Automation*, pp. 3315-3320, 2003.

[12] E. Marchand, F. Chaumette, and A. Rizzo, "Using the task function approach to avoid robot joint limits and kinematic singularities in visual servoing," in *Proc. IEEE/RSJ Int. Conf. Intelligent Robots and Systems*, pp. 1083-1090, 1996.

[13] F. Chaumette, and E. Marchand, "A new redundancy-based iterative scheme for avoiding joint limits: application to visual servoing," in *Proc. IEEE Int. Conf. Robotics and Automation*, pp. 1720-1725, 2000.

[14] A. Shademan, A. Farahmand, and M. Jagersand, "Robust Jacobian Estimation for Uncalibrated Visual Servoing," in *Proc. IEEE Int. Conf. Robotics and Automation*, pp. 5564-5569, 2010.

[15] H. Wang, Y.-H. Liu, and D. Zhou, "Adaptive visual servoing using point and line features with an uncalibrated eye-in-hand camera," *IEEE Trans. Robot.*, Vol. 24, no. 4, pp. 843-857, Aug. 2008.

Gon-Woo Kim He received M.S. and Ph.D. degrees from Seoul National University, Korea. He is currently an Associate Professor at Chungbuk National University. His research interests are visual servoing, mobile robot navigation and localization.